PNC TN941 74−42

5 th MEETING OF THE LIQUID METAL BOILING WORKING GROUP
GRENOBLE, APRIL 24-26, 1974

REVIEW OF THE JAPANESE WORKS ON LIQUID METAL BOILING

Yoshihiro KIKUCHI

POWER REACTOR AND NUCLEAR FUEL DEVELOPMENT CORPORATION
FBR SAFETY LABORATORY
OARAI ENGINEERING CENTER

動力炉・核燃料開発事業団 (Power Reactor and Nuclear Fuel Development Corporation)

CONTENTS

LOSS-OF-FLOW TESTS IN A SINGLE-PIN ANNULAR CHANNEL

Y. KIKUCHI, K. HAGA AND A. OHTSUBO
(Power Reactor and Nuclear Fuel Development Corporation)

Loss-of-flow tests have been conducted in an electrically heated single-pin annular channel. Each run was made by stopping the pump or closing the valve. The former simulates a pump coastdown accident and the latter a flow blockage.

The test section is shown in Fig. 1. The electrically heated pins fabricated in France were used for the present study. The maximum heat flux of the pins is 300 W/cm^2.

The test conditions are as follows:

Average heat flux	32 - 129 W/cm^2
Steady-state flow velocity	2.02 m/sec
Inlet temperature	352 - 424°C
Cover gas pressure	0.08 - 0.15 Kg/cm^{2}G

From the loss-of-flow tests the following has been concluded.

1. Incipient-Boiling Superheat

The effect of the rate of temperature rise on incipient-boiling (IB) wall superheat was investigated. Authors' data are shown in Fig. 2, compared with the results reported by Dwyer et al.[1] In the bulk boiling region, where the temperature ramp is less than 10°C/sec, the superheat is higher with increasing temperature ramp attaining the maximum value of 150°C. In the subcooled boiling region, however, where the ramp is greater than 10°C/sec, the superheat gradually decreases to the fixed value of approximately 80°C with increasing the ramp. This tendency may be attributed to the effect of natural convection turbulence. The natural convection may disturb the boundary layer near the heating surface with increasing temperature ramp[2] and depress the superheat.

2. Pressure Rise at Vaporization and Vapor Collapse

The pressure rise at the initial vaporization compared well with the vapor pressure corresponding to the IB wall superheat, as shown in Fig. 3.

The pressures that occur at the vapor collapse (due to the re-entry of the liquid column) correlate reasonably well with the re-entrant velocity of the liquid column. The measured values agree quite well with the theoretical values predicted from the sodium-hammer analysis, as shown in Fig. 4.

3. Void Pattern

In the earlier steady-state boiling tests under forced convection, the observed two-phase flow pattern was in the sequence of bubbly flow, slug flow and annular (mist) flow in sodium as in the case of water.[3] However, in the present loss-of-flow tests, the single-bubble slug-ejection pattern is dominant. The void pattern observed in the present tests agrees quite well with that calculated by the NAIS-P2 code[4] (single-bubble slug-ejection model), as shown in Fig. 5.

The initial expulsion acceleration of liquid is higher with higher IB wall superheat. The experimental results agree well with the theoretical predictions from the liquid-column analysis, as shown in Fig. 6.

4. Residual Liquid Film

The thickness (0.05 mm and 0.45 mm) of the residual liquid film becomes thinner with higher superheat, as shown in Fig. 7.

ACKNOWLEDGEMENT

The excellent heater pins for the present study were fabricated in the Nuclear Research Center of Grenoble, France. The authors wish to express their thanks to Dr. H. Mondin and his collaborators in the Center.

REFERENCES

1. O. E. Dwyer et al., "Incipient-boiling Superheats for Sodium in Turbulent Channel Flow: Effect of Rate of Temperature Rise," J. Heat Transfer (Series C of Trans. ASME), Vol.95 (1973) p.159 - p.165
2. See, for instance, I. Michiyoshi and Y. Kikuchi, "Buoyancy Effects on Forced Convection Flow and Heat Transfer," The Memories of the Faculty of Engineering, Kyoto University, Vol. 31, Part 3 (July 1969) p.363 - p.380 (in English)
3. Y. Kikuchi et al., "An Experimental Study of Steady-State Boiling of Sodium Flowing in A Single-Pin Annular Channel," J. Nucl. Sci. Technol. Vol. 11 (1974) (to be published)
4. Y. Kikuchi et al., "Incipient Boiling of Sodium Flowing in A Single-Pin Annular Channel," J. Nucl. Sci. Technol., Vol. 11, No. 5 (May, 1974) (to be published)

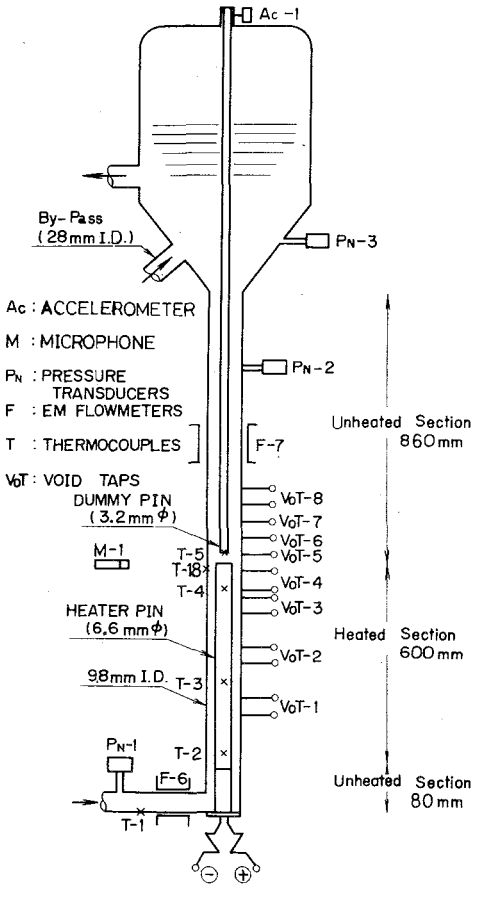

Fig. 1 Test Section

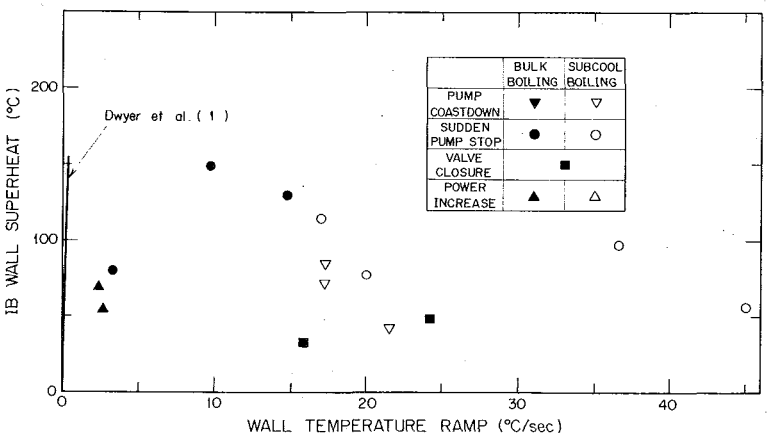

Fig. 2 Effect of rate of rise of wall temperature on IB wall superheat for loss-of-flow tests

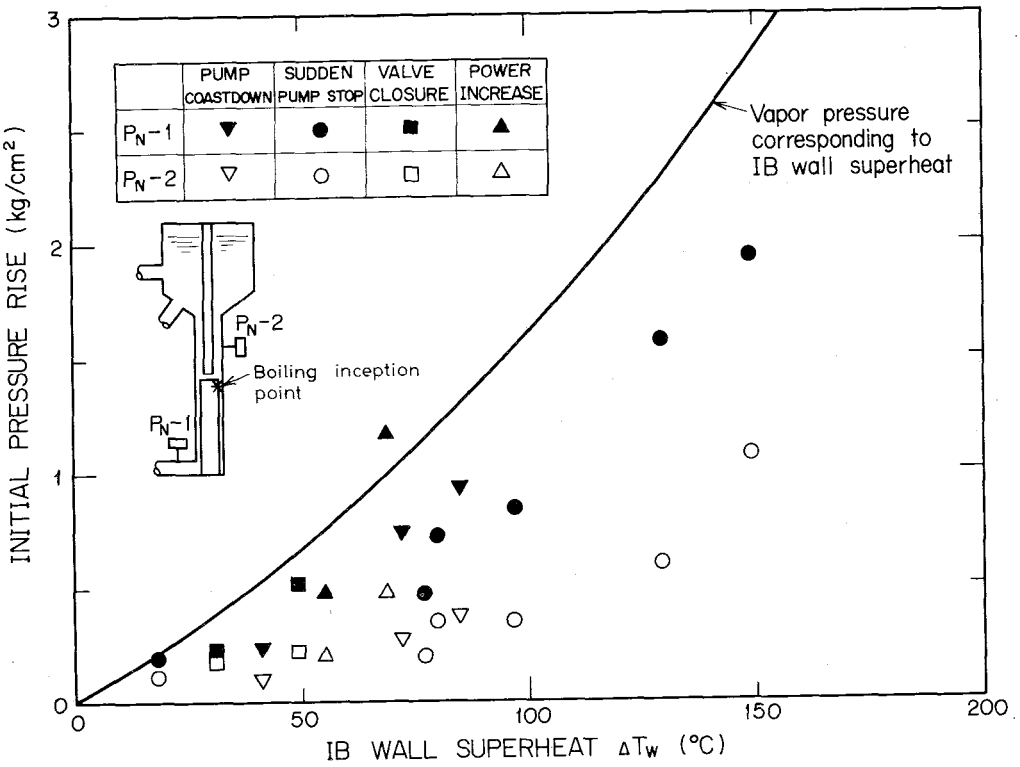

Fig. 3 Effect of IB wall superheat on initial pressure rise for loss-of-flow tests

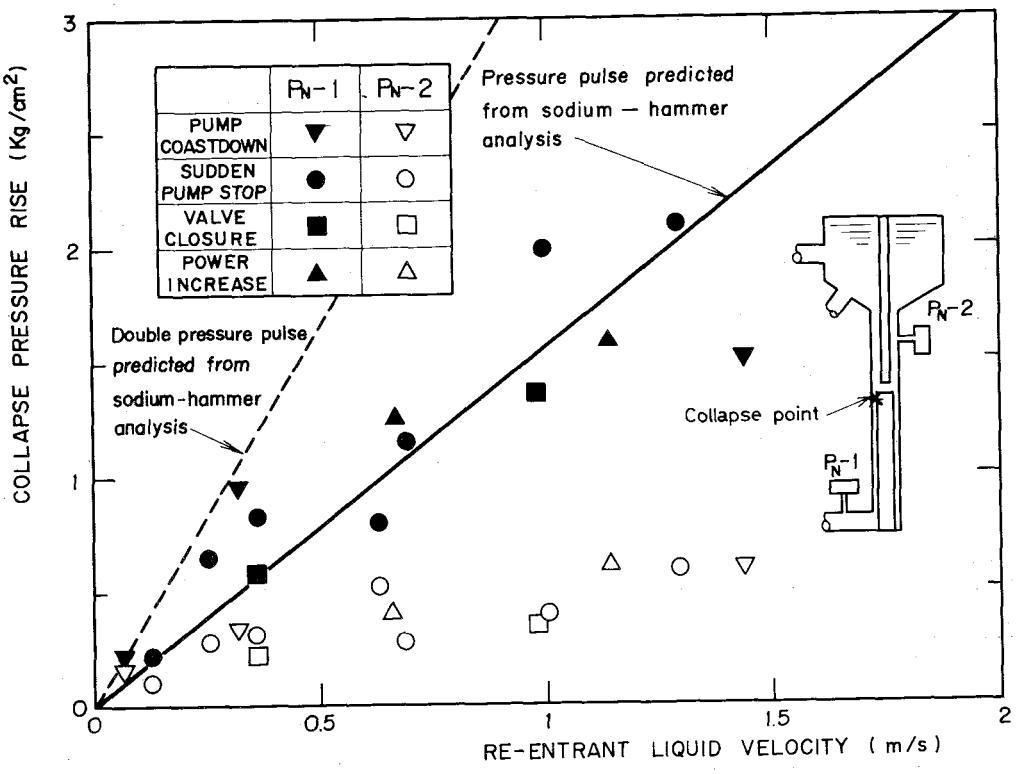

Fig. 4 Effect of re-entrant liquid velocity on pressure rise at vapor collapse for loss-of-flow tests

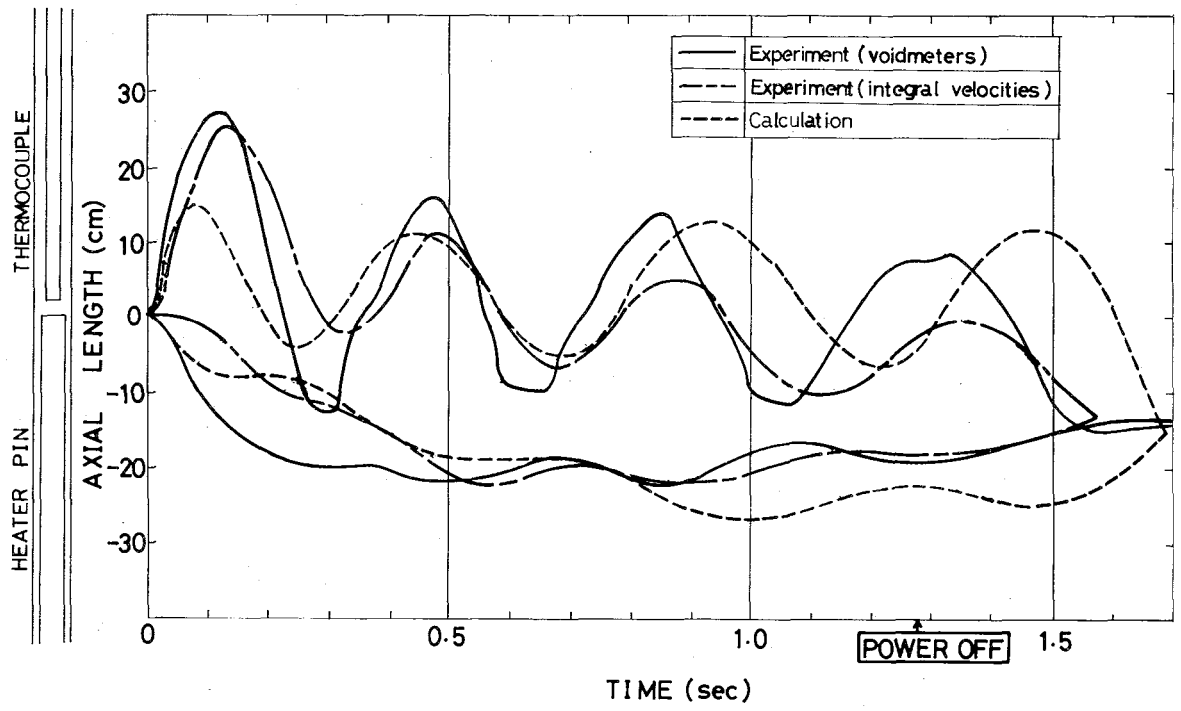

Fig. 5 Comparison of void pattern observed in the experiment FC-104 with that calculated by the NAIS-P2 code

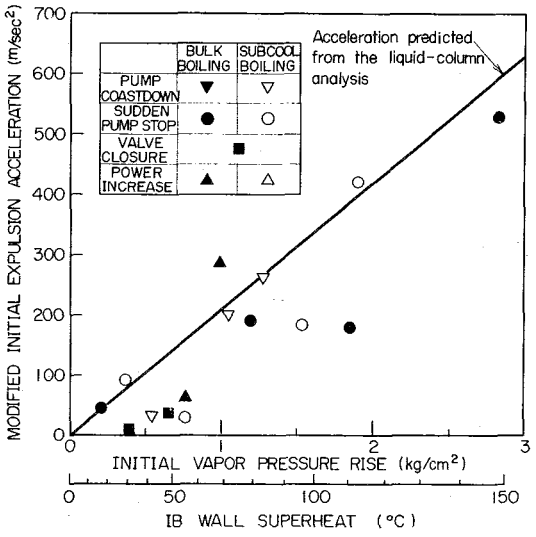

Fig. 6 Effect of initial vapor pressure rise corresponding to IB wall superheat on modified initial expulsion acceleration of liquid for loss-of-flow tests

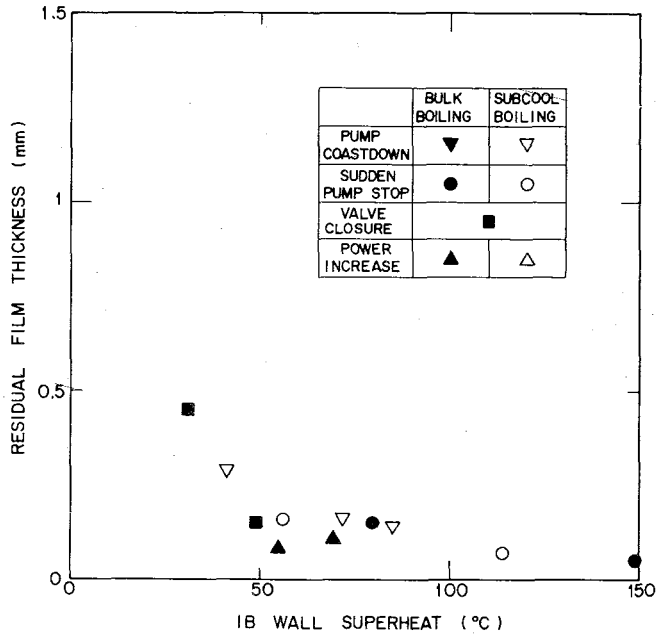

Fig. 7 Effect of IB wall superheat on thickness of residual liquid film for loss-of-flow tests

EXPERIMENTAL STUDIES OF SODIUM BOILING IN A SEVEN-PIN BUNDLE

Y. KIKUCHI, K. HAGA AND A. OHTSUBO
(Power Reactor and Nuclear Fuel Development Corporation)

The sodium boiling tests in a seven-pin bundle have recently been performed using the Sodium Boiling & Fuel Failure Propagation Test Loops SIENA located at PNC's Oarai Engineering Center. A schematic diagram of the loops is shown in Fig. 1.

Fig. 2 shows the test section with a seven-pin bundle. The length of the electrically heated pins (450 mm in heated length and 715 mm in gas plenum region) is approximately half of those for the Japanese LMFBR MONJU. The heaters manufactured in Sukegawa Electric Co., Ltd. were employed for the present study. The maximum heat flux of the heaters is 250 W/cm^2.

1. Loss-of-flow tests

12 test runs were carried out in order to provide experimental data on the voiding processes following the flow reduction at constant power. Each run was made by decreasing the inlet flow either slowly or abruptly. The experiments were carried out under the following conditions;

Average heat flux	34 - 64 W/cm^2
Steady-state flow velocity	0.95 - 1.20 m/sec
Inlet temperature	430 - 519°C
Cover gas pressure	0.03 - 0.06 Kg/cm^2G

The typical results are shown in Fig. 3 and Fig. 4. Because of the large radial temperature gradient in the bundle, the coolant voiding is initially limited to the center of the bundle and then spreads slowly. In order to describe these voiding processes, the experimental results are being compared with the prediction by the computer code SPACE (two-dimensional voiding model).

2. Steady-state boiling tests

Steady-state boiling tests were conducted at low pressure head and low heat flux. After the boiling inception, the heat flux was further increased step by step until the dryout occurred.

Fig. 5 shows the typical results of steady-state boiling. In the local boiling region, no flow instability is observed because the subchannels near the wrapper wall are still filled with subcooled liquid. The pressure drop appears to remain constant. In the bulk boiling region, considerable upstream voiding occurs and then the inlet flow is reduced. The inlet flow reversal occurs resulting in the final dryout of the pins.

The larger-scale experiments in a 19-pin bundle will be scheduled for next year.

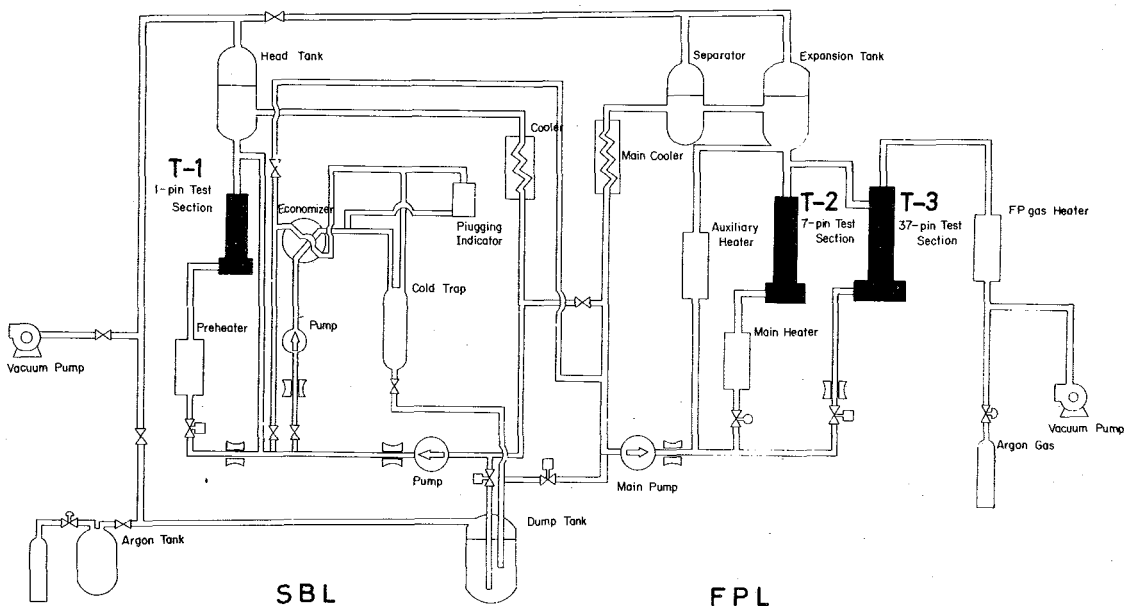

Fig. 1 Flow diagram of Sodium Boiling Test Loop & Fuel Failure Propagation Test Loop SIENA

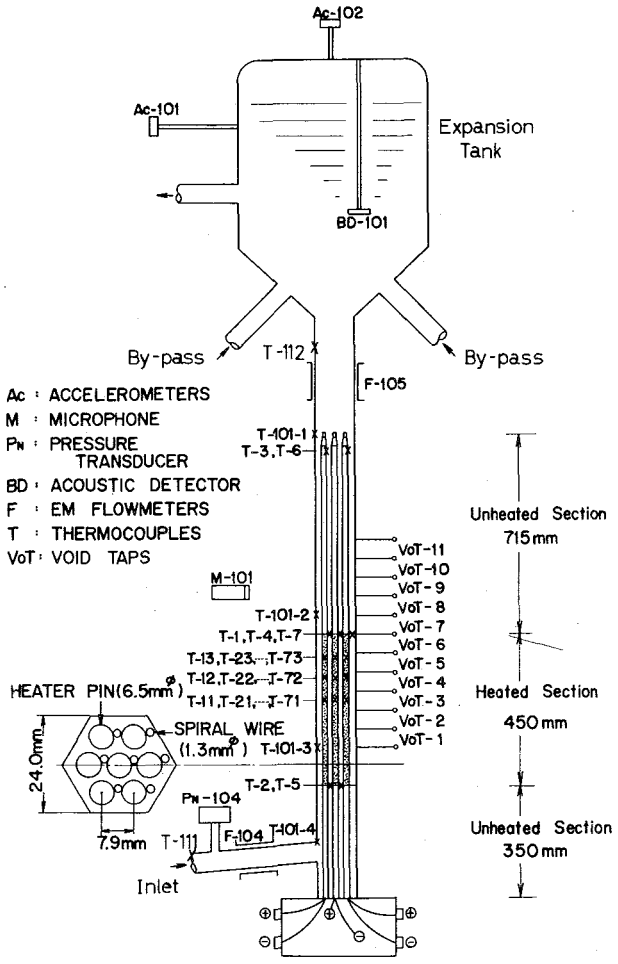

Fig. 2 Test section with a 7-pin bundle

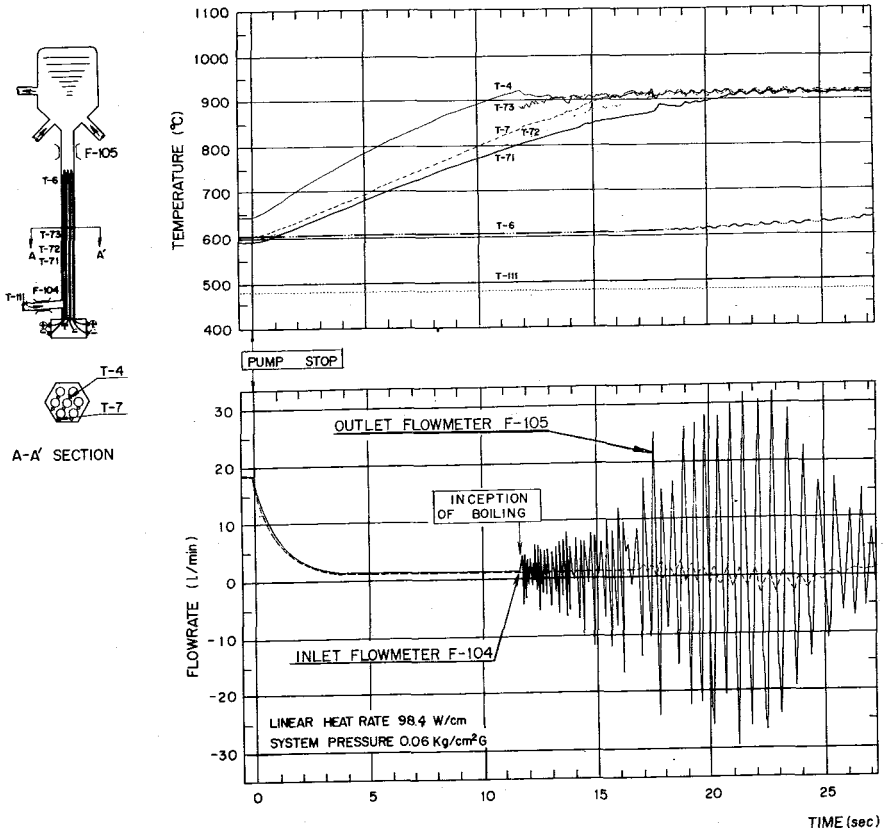

Fig. 3 Signals of temperatures and flowmeters for a loss-of-flow test in 7-pin bundle (Test No. 7FC-105)

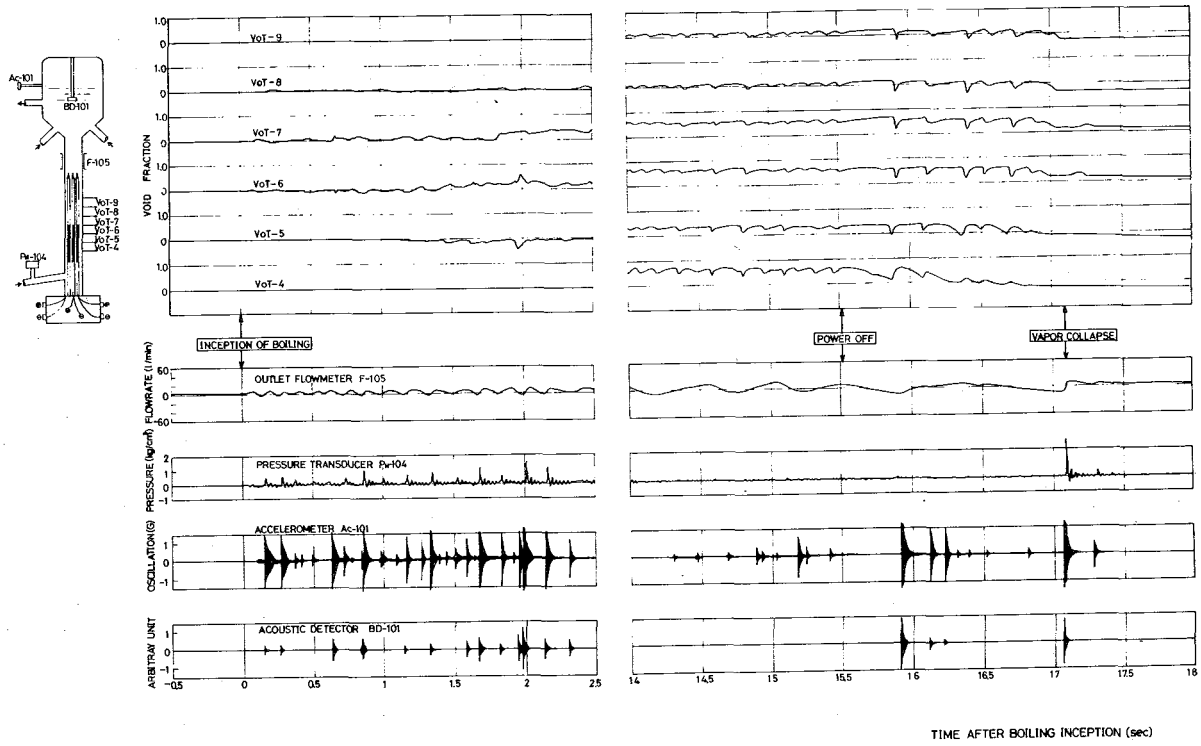

Fig. 4 Signals of void meters, flowmeter, pressure transducer, accelerometer and acoustic detector for a loss-of-flow test in a 7-pin bundle (Test No. 7FC-105)

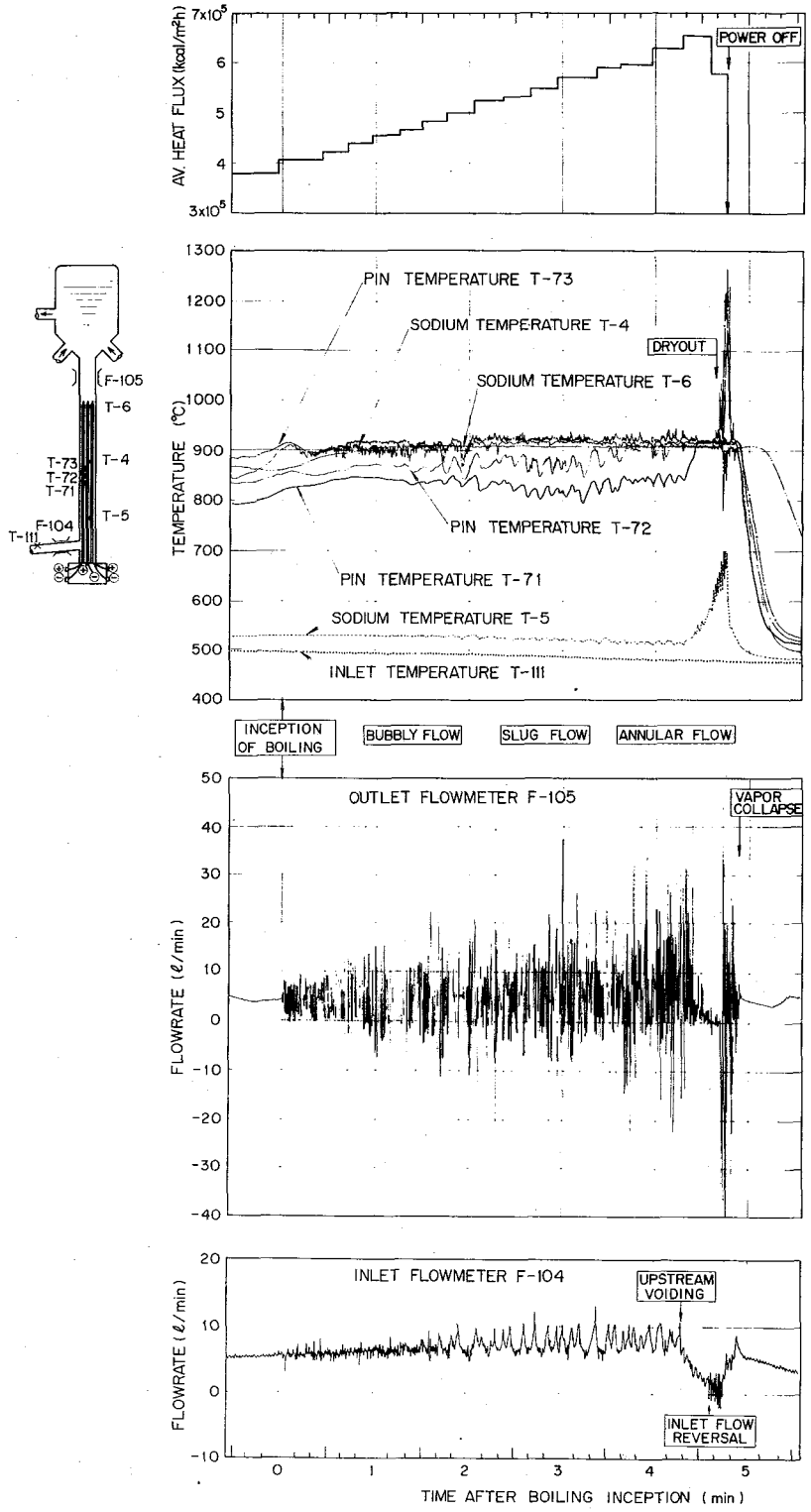

Fig. 5 Signals of temperatures and flowmeters with heat flux for steady-state boiling in a seven-pin bundle (Test No. 7B-106)

ACOUSTIC NOISE ASSOCIATED WITH FORCED-CONVECTION SODIUM BOILING IN A SINGLE-PIN ANNULAR CHANNEL

Y. KIKUCHI, K. HAGA AND T. TAKAHASHI
(Power Reactor and Nuclear Fuel Development Corporation)

1. INTRODUCTION

It is explained in a number of published studies that the characteristics of acoustic noise with boiling can serve as an indicator of the intensity of the boiling process and also can be used for controlling the operation of heat exchangers. In particular, anomalous coolant boiling should be detected at its incipient stage in no-boiling liquid-cooled reactors, especially in LMFBRs since the coolant boiling could lead to the total core failure. Various methods are proposed for the detection of boiling, but the measurement of acoustic noise signals associated with boiling phenomenon seems most promising.[1]

However, in order to utilize acoustic signals for these purposes it is first necessary to know the manner in which their characteristics (frequency spectrum, intensity) depend on the principal variables of the boiling process, which are heat flux, pressure and subcooling. The effect of the heat flux on the noise intensity was investigated in published studies[2,3,4] and it can be presently regarded as reliable that the intensity first rises sharply, and then remains virtually constant. The frequency spectrum changes little. The effect of pressure and subcooling on the acoustic noise is presented by Kichigin and Povsten.[5] But these studies were carried out of pool boiling of ordinary nonmetallic liquids, especially water. There are little data, to authors' knowledge, on liquid-metal boiling.

In order to make these problems clear, authors carried out a study of the effect of heat flux on the intensity and frequency spectrum of acoustic noise associated with boiling of sodium under forced convection.

2. INSTRUMENTATION SYSTEM

Fig. 1 shows the instrumentation and data processing system for acoustic noise signals. The system was assembled for detecting, conditioning, recording, and analyzing the acoustic signals with boiling.

A microphone was set outside the test section for the present study as shown in Fig. 2. The Sony Model ECM-21 microphone had a flat response up to 40 kHz. This sensor was equipped with a tapecorder. The Sony Model 9540 tapecorder was used for recording, storage, and reproducing of the boiling acoustic noise signals. The maximum frequency limit of 20 kHz was attainable with the tape speed of 9.5 cm/sec. The Pionear Model SE-100 headphone was used for monitoring the acoustic noise.

A Rion Model SA-21 1/3 octave real-time spectrum analyzer was used for the spectral measurements. This unit has a frequency range from 44.5 Hz to 22.4 kHz. The spectral display appears on the screen of a cathode ray tube with frequency of the applied signal displayed on the horizontal axis, while the intensity of the signal is displayed on the vertical axis. The frequency display is logarithmic.

A NF Circuit Model M-172TA AC voltmeter was used for measuring the acoustic intensity conditioned by a Multimetrics Model AF-120 active filter. The AC voltmeter has a frequency range from 5 Hz to 2 MHz.

3. SPECTRUM OF ACOUSTIC NOISE

Fig. 3 shows the frequency spectra of acoustic noise with boiling as well as without boiling in the steady-state boiling test No. B-102. It can be seen that the frequency spectra are very similar in shape but that the boiling causes a considerable increase in intensity at all frequencies. Distinct peaks are also observed in kilohertz range for all the measurements especially with boiling. These peaks may be characteristic to resonances of the test section system and/or the microphone.[6]

From these facts, it will be seen that spectral analysis reveals little information about boiling since boiling causes a general rise in intensity at all frequencies. It follows therefore that to perform a spectral analysis in the case is undesirable as it increases the measurement time considerably. It would seem to be much more reasonable to relay on wide-band intensity measurements, whereupon the increase in bandwidth can be used to reduce measurement time without sacrifice of accuracy.

4. INTENSITY OF ACOUSTIC NOISE

Fig. 4 shows the effect of the average heat flux q_{AV} on the intensity ratio I/Io in the steady-state boiling test No. B-102, where I is the noise intensity at given flux q_{AV} and Io is the noise intensity without boiling. Each curve is plotted as the acoustic intensity conditioned by the high-pass filter indicated in the figure. From the figure it is seen that at any high-pass filter the acoustic intensity with boiling first increases sharply with rise in the heat flux and then, upon attaining the maximum, decreases somewhat to remain constant. This manner is indicated more clearly with higher cut-off frequency of high-pass filter.

The first boiling state, as long as the intensity does not attain its maximum, is considered to be developing nucleate boiling, that is mainly the bubbly flow region. The fully developed boiling state, after the intensity attains its maximum, is considered to be the slug flow and annular flow region.

From these facts, it will be seen that wide-band intensity measurements are much suitable for use in operation of the reactor (initiation of an alarm, reactor power reduction, etc.) since the mainly low-frequency hydrodynamic noise and pump noise can be eliminated with a high-pass filter in order to achieve a favorable signal to intensity ratio.

ACKNOWLEDGEMENT

The authors wish to express their thanks to Dr. H. Mondin and his collaborators in the Nuclear Research Center of Grenoble, France, who kindly offered their excellent heater pins for the present study.

REFERENCES

1. T. T. Anderson et al., "Survey and Status Report on Application of Acoustic-Boiling-Detection Techniques to Liquid-Metal-Cooled Reactors," ANL-7469, (1970).
2. M. F. M. Osborne and F. H. Holland, "The Acoustical Concomitants of Cavitation and Boiling, Produced by a Hot Wire (I)," J. Acoust. Soc. Amer. Vol. 19, (Jan. 1947) PP.13-20.
3. F. L. Schwartz and L. G. Siler, "Correlation of Sound Generation and Heat Transfer in Boiling," Trans. ASME, J. Heat Transfer, Vol. 87, Ser. C, (Nov. 1965) PP.436-438.

4. L. C. James, "Experiments on Noise as an Aid to Reactor and Plant Operation," Nucl. Eng. Vol. 10 (Jan. 1965) PP.18-22.
5. A. M. Kichigin and S. G. Povsten, "Effect of Pressure and Subcooling on the Nature of Noise in Pool Boiling of Liquids," Fluid Mechanics-Soviet Research, Vol. 2, No. 3 (1973) PP.154-157.
6. H. Nishihara, "Resonant Acoustic Noise Spectra of Nucleat Coolant Boiling," J. Nucl. Sci. Technol., Vol. 11, No. 1 (1974) PP.1-7.

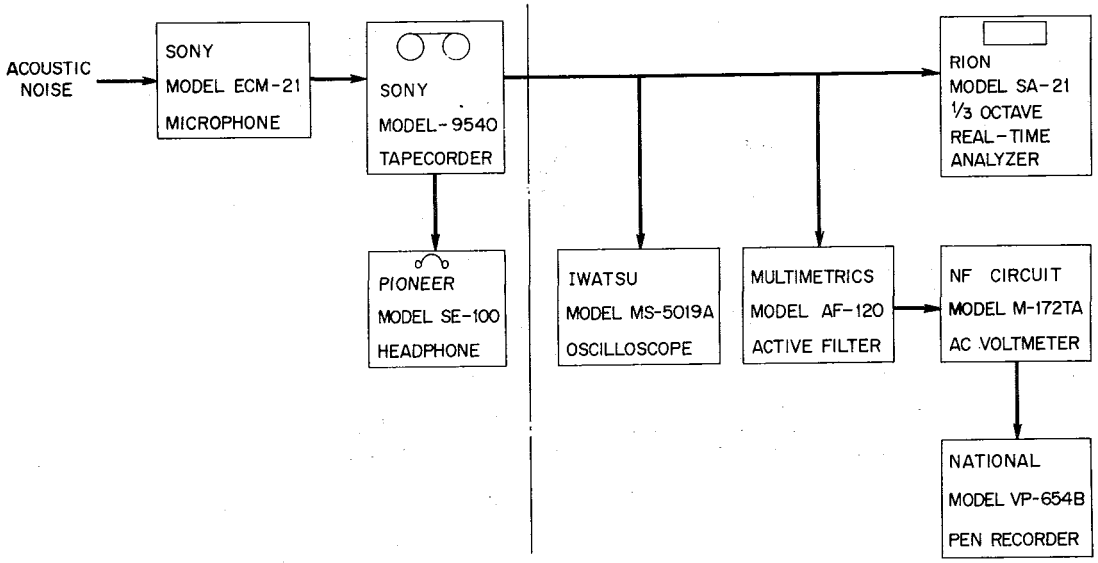

Fig. 1 Instrumentation and data processing system for acoustic boiling noise signals

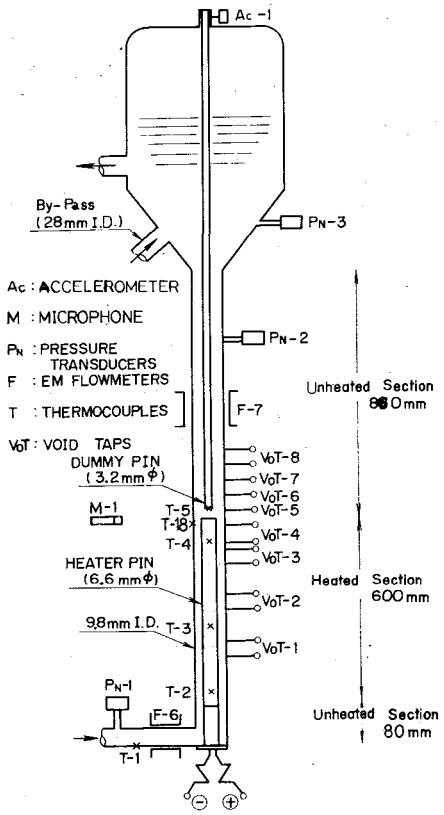

Fig. 2 Test section

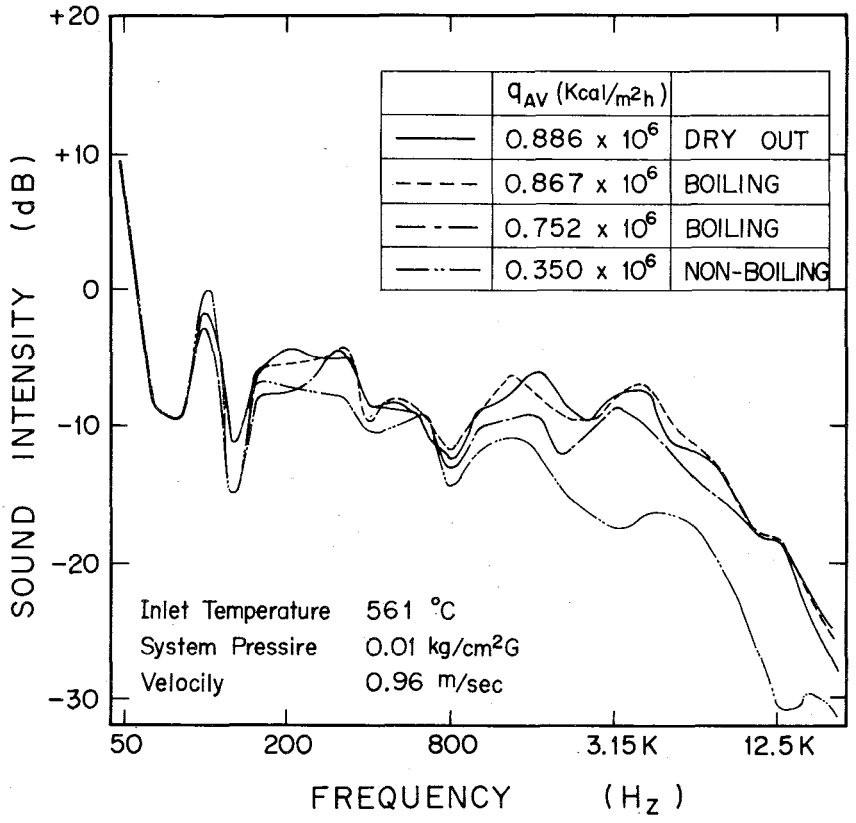

Fig. 3 Frequency distribution of sound intensity in boiling for state boiling test B-102

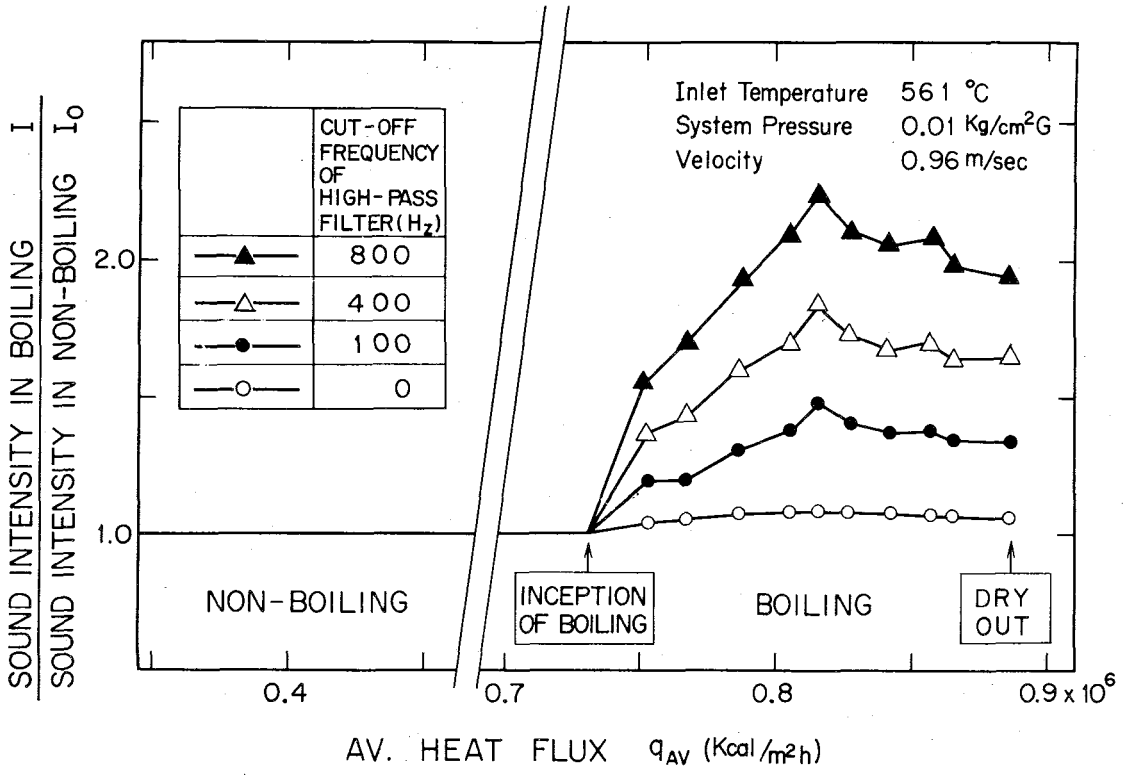

Fig. 4 Effect of average heat flux on sound intensity in boiling for steady-state boiling test B-102

THE EFFECTS OF BOWING DISTORTIONS ON HEAT TRANSFER IN A SEVEN-PIN BUNDLE

Y. DAIGO, A. OHTSUBO, K. HAGA AND Y. KIKUCHI
(Power Reactor and Nuclear Fuel Development Corporation)

Experimental studies have been conducted of heat transfer in sodium flowing in an electrically heated seven-pin bundle where two pins were bowed to form a point contact.

Fig. 1 shows the test section with a bowed bundle. Each pin has 6.5 mm in diameter and 450 mm in heated length (approximately half length of MONJU's fuel pin). The bundle is tightly packed with 1.3 mm dia. wire wrap spacers and placed in a hexagonal flow duct. The pitch-to-diameter ratio (P/D) is 1.22. The center pin is bowed symmetrically 264.3 mm long and the maximum bowed point contacts with a outer normal pin.

The experimental conditions are as follows:

Average heat flux	7 - 59 W/cm^2
Flow velocity	0.4 - 5.2 m/s
Inlet coolant temperature	320 - 400°C

Fig. 2 shows the measured clad temperature difference across the bowed pin bundle. In order to compare with the bowed pin bundle, the experimental results of the normal pin bundle are also indicated in the figure. The hot spot is observed at the contact point for the region of low velocities, but for the region of higher flow velocities (than 2.7 m/s) the hot spot is at the downstream from the contact point.

The experimental results are being compared with the calculation by the PICO code in which the local temperature rise around the point of contact is calculated.

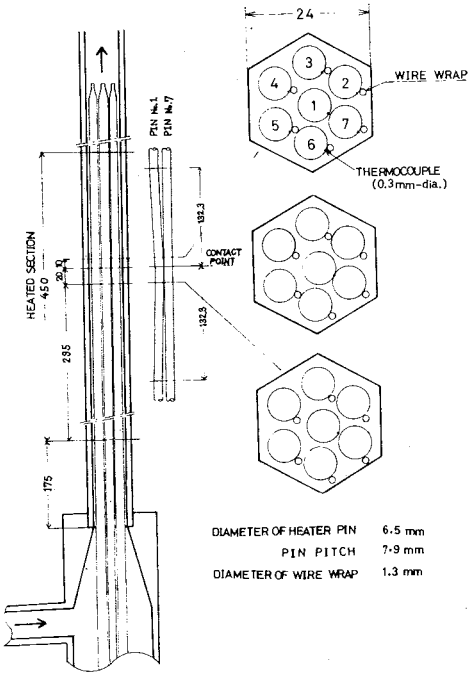

Fig. 1 Test section with a bowed pin bundle

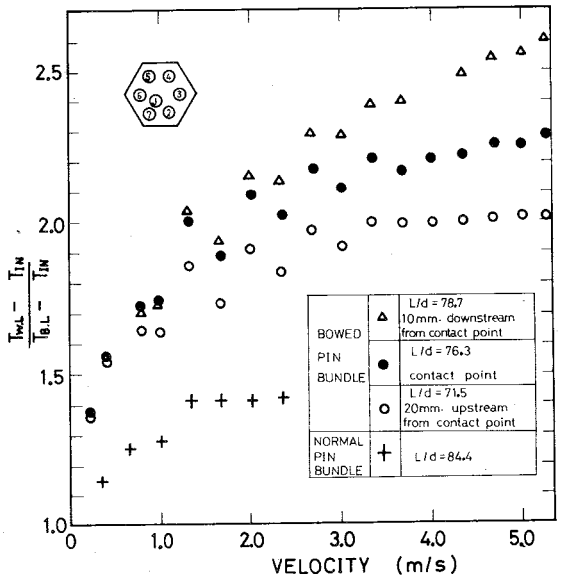

Fig. 2 Effect of velocity on wall temperature

SPACE: A TWO-DIMENSIONAL HYDRODYNAMICS CODE FOR THE FBR ACCIDENT ANALYSIS

H. YOKOZAWA AND H. NAKAGAWA
(Tokyo Electric Power Co., Inc.)

The local blockage or the sodium boiling in the FBR subassembly comes to the fuel pin overheat. In order to define the coolant and sodium void behavior in the subassembly, multi-dimensional analysis of non-compressible fluid is required. The two-dimensional code, SPACE, is available for the transient analysis of sodium voiding.

1. Description of the SPACE code

The equation of motion for the non-compressible viscous fluid, in the cylindrical co-ordinates, is

$$\frac{\partial V_r}{\partial t} + V_r\frac{\partial V_r}{\partial r} + V_z\frac{\partial V_r}{\partial Z} = X_r - \frac{1}{\rho}\frac{\partial P}{\partial r} + \nu\left(\frac{\partial^2 V_r}{\partial r^2} + \frac{1}{r}\frac{\partial V_r}{\partial r} + \frac{\partial^2 V_r}{\partial Z^2} - \frac{V_r}{r^2}\right)$$

$$\frac{\partial V_z}{\partial t} + V_r\frac{\partial V_z}{\partial r} + V_x\frac{\partial V_z}{\partial Z} = X_z - \frac{1}{\rho}\frac{\partial P}{\partial Z} + \nu\left(\frac{\partial^2 V_z}{\partial r^2} + \frac{1}{r}\frac{\partial V_z}{\partial r} + \frac{\partial^2 V_z}{\partial Z^2}\right)$$

The equation of continuity is

$$\frac{1}{r}\frac{\partial}{\partial r}(rV_r) + \frac{\partial V_z}{\partial Z} = 0$$

X_r and X_z represent the radial component and the axial component respectively, of external forces: 1) gravitional force, 2) frictional resistance due to the fuel pin bundle and the wrapper tube, 3) external pressure (inlet or outlet pressure and void pressure), 4) surface tension of of the void. The sodium is heated from the fuel pins, and thermal energy is transfered by the sodium flow. The energy equation of the sodium is

$$\frac{\partial T}{\partial t} = \frac{h}{\rho C_p}(T_f - T) - \frac{1}{r}\frac{\partial}{\partial r}(rV_r T) - \frac{\partial}{\partial Z}(V_z T)$$

A sodium void is formed at the central channel of the subassembly under the following condition,

$$P_{sat}(\Theta(r,Z) - \Delta\Theta_{sup}) \geq P(r,Z)$$

The mass flow density of sodium vapor is expressed in the following equation, considering its vaporization and condensation on the fuel pin surface.

$$\mu = k\left(P_f / \sqrt{\frac{8}{\pi}R\Theta_f} - P_v / \sqrt{\frac{8}{\pi}R\Theta_v}\right)$$

The sodium liquid around the void is expelled in the radial direction as well as in the axial direction by the vapor pressure. The two-dimensional calculation on the homogeneous hydraulic model may explain the realistic flow regime.

2. Calculated results

The pressure distribution surrounding the sodium void depends substantially on the dimensions of the sodium void and the wrapper tube. Figure 1 shows a calculated result of the sodium voiding in a subassembly

during the loss-of-flow accident. It is seen that a considerable amount of sodium liquid remains near the wrapper tube. The liquid would delay the fuel failure propagation. The pressure distribution are shown in Fig. 2. The velocity distribution of the sodium flow is shown in Fig. 3.

3. Conclusion

The SPACE code based on a two-dimensional non-compressible flow model was developed to calculate the behavior of the viscous fluid and its void. It was made clear that the accident analysis in FBR subassembly requires the multidimensional numerical calculation because a considerable liquid remained near the wrapper tube would be effective to delay the fuel failure propagation. The SPACE code will further give a preliminary knowledge of the molten fuel to sodium interaction.

In order to quantitize the delay of fuel failure propagation, the experimental verification is being done in a seven-pin bundle geometry at PNC's Oarai Engineering Center.

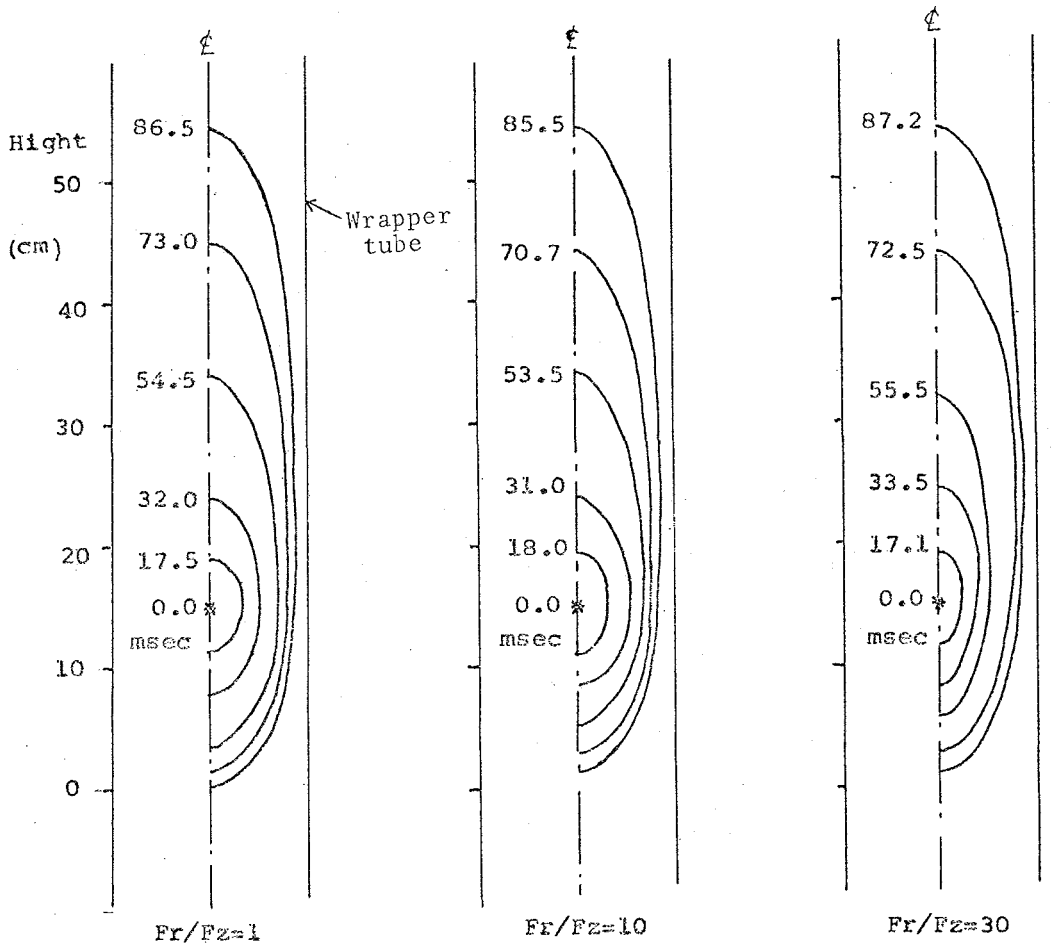

Fig. 1 Two-dimensional voiding in a subassembly during a loss-of-flow accident (in a case of channel blockage)

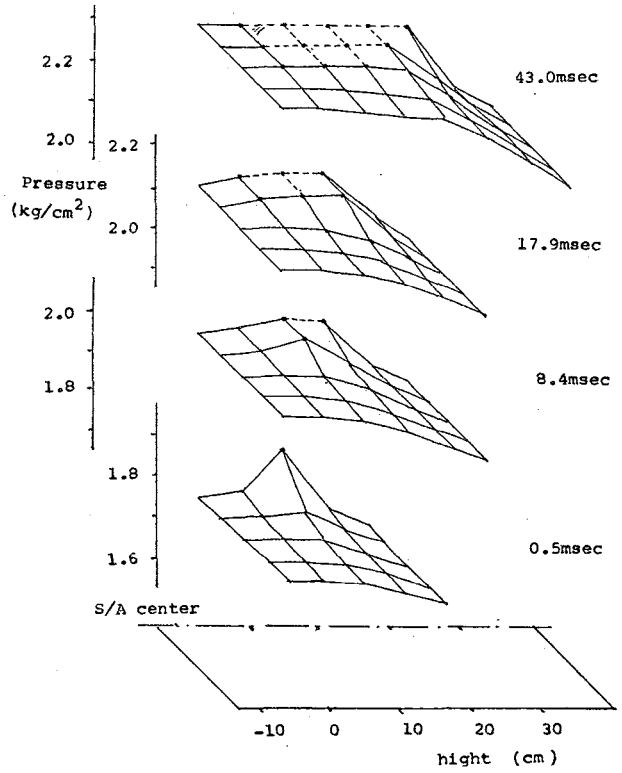

Fig. 2 Pressure distribution in a subassembly during sodium boiling

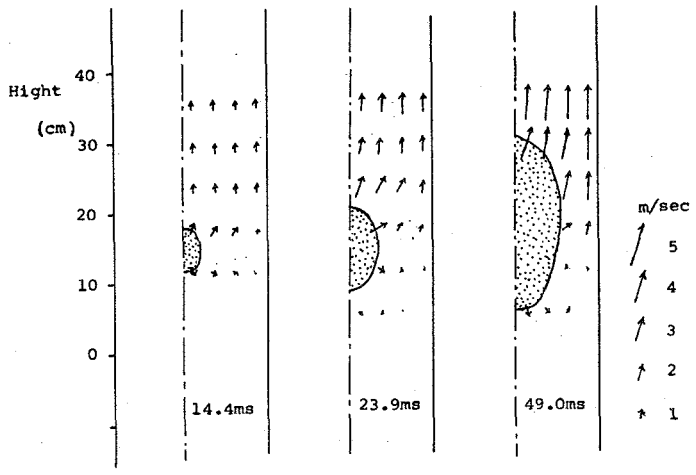

Fig. 3 Flow velocity distribution in a subassembly during sodium boiling

CRUSH & FYNAM: A COMPUTER CODE FOR THE ANALYSIS OF FAST REACTOR ACCIDENTS

H. YOKOZAWA, H. NAKAGAWA
(Tokyo Electric Power Co., Inc.)
and R. TAKAHASHI
(Tokyo Institute of Technology)

The CRUSH & FYNAM code predicts the accident behavior, especially sodium boiling and fuel melting, in fast reactors. The modified code for allowing multiple bubbles at the same time, gives the satisfactory results to analyse the accident of reactivity insertion, pump coast down and channel blockage.

The FBR core accidents, such as shown in Fig. 1, bring about sodium boiling and fuel melting. The CRUSH code describes the ejection and collapse of multiple bubbles in the channel, considering the movement of residual liquid film and the dryout of fuel pin. The FYNAM code describes the movement of molten fuel due to the fission product's vaporization.

The geometry of the single channel treated in the CRUSH code is shown in Fig. 2.

Figure 3 shows the fuel surface temperature. It is seen the fuel temperature is affected by the residual liquid film.

Figure 4 shows the channel voiding and the film thickness. The fuel surface which is once dried out is wetted again with the liquid expelled by the second void.

Experimental verifications of this model are being done by the out-of-pile experiments simulating flow coast down condition at PNC's Oarai Engineering Center.

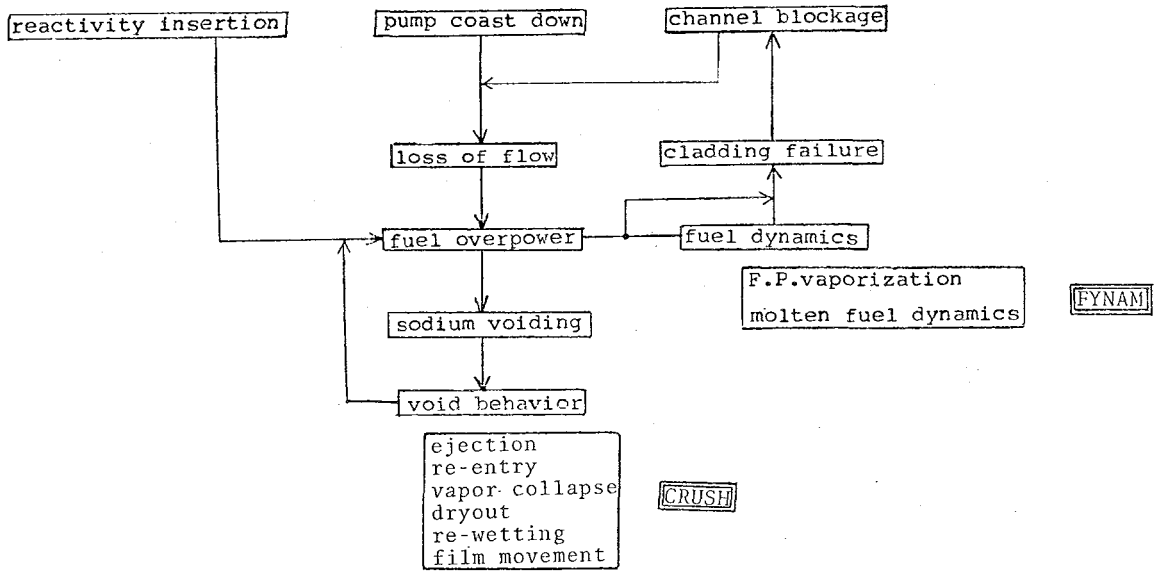

Fig. 1 Accident process treated in the CRUSH & FYNAM code

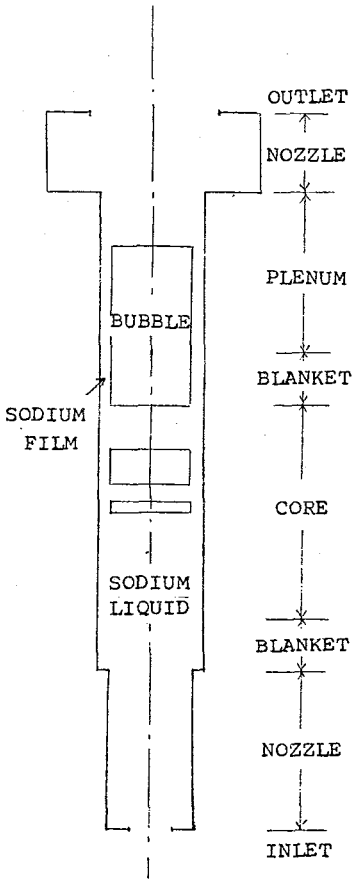

Fig. 2 Geometry of single channel

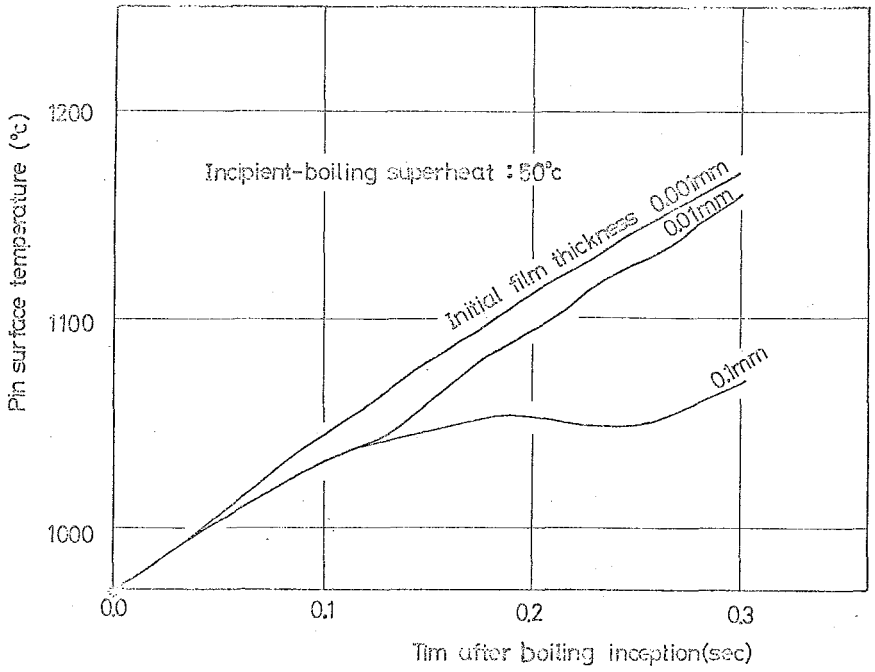

Fig. 3 Effect of initial thickness of residual liquid film on temperature rise of pin surface

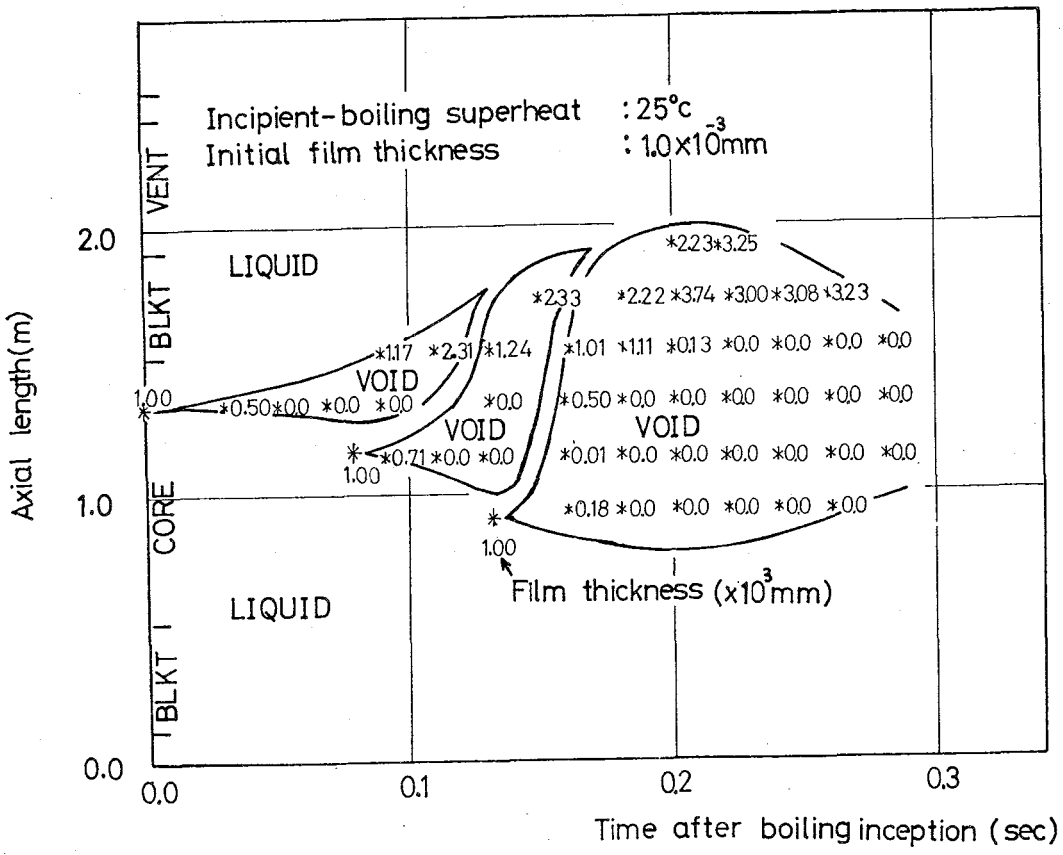

Fig. 4 Channel voiding during a flow coastdown accident